

# Electron quantum optics in quantum Hall edge channels

Charles Grenier,<sup>1</sup> Rémy Hervé,<sup>1</sup> Gwendal Fève,<sup>2</sup> and Pascal Degiovanni<sup>1,\*</sup>

<sup>1</sup>*Laboratoire de Physique, Ecole Normale Supérieure de Lyon  
46 allée d'Italie, 69007 Lyon, France*

<sup>2</sup>*Laboratoire Pierre Aigrain, Ecole Normale Supérieure  
24 rue Lhomond, 75005 Paris, France*

In this paper, we review recent developments in the emerging field of electron quantum optics, stressing analogies and differences with the usual case of photon quantum optics. Electron quantum optics aims at preparing, manipulating and measuring coherent single electron excitations propagating in ballistic conductors such as the edge channels of a 2DEG in the integer quantum Hall regime. Because of the Fermi statistics and the presence of strong interactions, electron quantum optics exhibits new features compared to the usual case of photon quantum optics. In particular, it provides a natural playground to understand decoherence and relaxation effects in quantum transport.

Keywords: quantum transport, quantum Hall effect, quantum coherence, quantum optics

## Introduction

The development of quantum optics started in the 50s and 60s, motivated by the need to understand photodetection, statistics and coherence of light within the framework of quantum theory. In the late 50s, the seminal Hanbury-Brown and Twiss (HBT) experiment<sup>1,2</sup> demonstrated the bunching of photons emitted by a classical chaotic source and stimulated the development of the quantum theory of optical coherences by Glauber<sup>3-5</sup>. An important milestone in quantum optics was the demonstration of the non-classical character of fluorescence radiation emitted by a single atom<sup>6</sup> and, later, the demonstration of photons sources showing photon antibunching<sup>7,8</sup>. As can be seen from a recent review<sup>9</sup>, a variety of single photon sources have been demonstrated: some of them are based on single molecules<sup>10</sup> or colored centers in diamond<sup>11</sup> and others on artificial nanostructures such as quantum wells<sup>12</sup> or quantum dots in microcavities<sup>13</sup>. Such sources are used to implement quantum key distribution protocols. An important effort is now oriented towards reliable high rate sources of entangled photon pairs<sup>14,15</sup> in the perspective of quantum communication protocols<sup>16</sup>. Since Glauber's seminal papers, a lot of work has been devoted to the production and characterization of quantum states of the electromagnetic field. In particular, spectacular results in the preparation and measurement of the quantum state of an electromagnetic field in the microwave domain have been achieved in cavity QED, either using Rydberg atoms in ultrahigh finesse superconducting cavities<sup>17</sup> or using superconducting nanocircuits. In this latter stream of research, known as circuit QED<sup>18</sup>, recent progresses have been spectacular, including for example the generation of arbitrary quantum states up to 12 photons in a cavity<sup>19</sup>.

Following this historical trend, progresses in mesoscopic physics have increasingly brought closer the dream of performing quantum optics like experiments with electrons in condensed matter systems where many body effects are expected to play a crucial role. During the last twenty years, electronic interferences observed in conductance measurements routinely provided information about first order electron coherence, although the use of quantum optics language was not emphasized. This recently culminated with Mach-Zehnder experiments performed on edge channels of high mobility 2DEG in the integer quantum Hall effect regime<sup>20</sup>, showing large coherence lengths in excess of 10  $\mu\text{m}$  at low temperature<sup>21</sup>.

Following a parallel path with optics, in the beginning of the 90s, theoreticians proposed to investigate intensity fluctuations of the electrical current<sup>22-25</sup> such as shot noise, a manifestation of electron granularity first pointed out by W. Schottky<sup>26</sup>. The analogy between electronic quantum shot noise and photon noise was soon established and the importance of studying current correlations in the spirit of Hanbury Brown and Twiss became evident<sup>24,25</sup>. In 2007, following a proposal by Samuelsson, Sukhorukov and Büttiker<sup>27</sup>, Heiblum and his collaborators demonstrated two particle interferences in quantum Hall edge channels<sup>28</sup>.

These considerations emphasized the interest for realizing “electron quantum optics” experiments but it is only recently that the fine control of electron dynamics and high frequency current noise measurements at relevant time-scales have been achieved<sup>29</sup>. A further breakthrough has been brought recently with the experimental realization of

---

\*To appear in the proceedings of StatPhys 24 satellite conference on *International Conference on Frustrated Spin Systems, Cold Atoms and Nanomaterials* held in Hanoi (14-16 July 2010).

an on demand single electron source<sup>30,31</sup>. By opening the way to experiments involving single electrons instead of the flow continuously emitted from a voltage biased contact, this source offers totally new opportunities.

In this context, an important and natural question is to understand how far the analogy between “electron quantum optics” and photonic quantum optics can go? The Fermi statistics of electrons is expected to bring in new features. First of all, the ground state of a metallic conductor is a Fermi sea which, as we shall see, radically differs from the electromagnetic vacuum. Moreover, even in the absence of interactions, Fermi statistics leads to radically different phenomenon than in optics: for example, with fermions, entanglement production from sources at equilibrium is possible even in the absence of interactions whereas this is prohibited for bosonic particles such as photons<sup>32</sup>.

Besides quantum statistics, Coulomb interactions have strong consequences on the propagation and coherence of electronic excitations within a ballistic conductor. Although one expects the Pauli exclusion principle to block inelastic processes at low energies, the quantum optics paradigm of freely propagating particles is seriously questioned in electronic systems. A crucial question is thus not only to understand the effects of quantum statistics, but also deviation from the non-interacting picture due to electron-electron interactions and to decoherence induced by the electromagnetic environment<sup>33–35</sup>.

Here we review some of the recent developments in the emerging field of electron quantum optics, stressing analogies and differences with the case of quantum optics with photons. Although the ultimate goal of electron quantum optics would be to study and manipulate in a controlled way the quantum state of electrons in conductors, it should be remembered that, compared to the usual case of photon quantum optics, this field is still very young. Although several groups are now working in this field, only a few electron quantum optics experiments have been performed compared to what has been achieved in photon quantum optics. Thus, even if this review mainly focuses on theoretical aspects, we have chosen to restrict ourselves to the discussion of topics directly related to forthcoming experimental projects which include the analogous of the famous Hanbury Brown & Twiss and Hong, Ou, Mandel experiments as well as quantitative studies of electron decoherence in quantum Hall edge channels.

In section I, the basic notions needed to characterize electron quantum coherences are introduced and the parallel with quantum optics is made explicit. Then, in section II, we discuss how single electron coherence can be measured thus leading to a quantum tomography protocol for single electrons in quantum Hall edge channels. Finally, in section III, we discuss electron decoherence and relaxation making an explicit and somehow surprising connexion between this problem and high frequency electric transport.

## I. ELECTRON COHERENCE

So far, experiments have been performed using phase-coherent ballistic conductors realized using high mobility 2D electron gases in the integer quantum Hall regime. Then, electron propagation takes place within chiral edge channels<sup>36</sup> suitable to mimic quantum optics setups<sup>37</sup>. Having in mind these experimental realizations, our discussion will be focused on chiral edge channels. Although this may sound restrictive, we stress that these systems already provide many of the components needed for quantum optic experiments: sample edges are perfect mirrors whereas the quantum point contact<sup>38</sup> provides the analogous of a beam splitter for electrons<sup>39</sup>. Moreover, the single electron source has been recently demonstrated<sup>30,31</sup> and powerful noise measurement techniques have been developed<sup>40,41</sup>.

### A. From photons to electrons

In quantum optics, quantum coherence properties of photons are described by Glauber correlation functions which are closely related to photodetection signals<sup>3,4</sup>. Photodetection is the conversion of a photon into an electrical signal. An old example is provided by the photomultiplier which relies on the photoelectric effect to convert a single photon into a single electron and then amplifies the corresponding current using secondary emission of electrons in dynodes. Modern photodetectors in the optical domain are photodiodes among which single photon avalanche photodiodes. These solid state photodetectors reach single photon sensitivity and have a photon arrival time resolution of a few tens of picoseconds<sup>42</sup>.

Using time dependent perturbation theory, the photodetection signal of a single photodetector at position  $x$  can be expressed in term of two correlation functions:

$$I_D(t) = \int \mathcal{G}_\rho^{(1)}(x, \tau; x, \tau') K_D(\tau, \tau') d\tau, d\tau' \quad (1)$$

where the first order correlation function  $\mathcal{G}_\rho^{(1)}(x, \tau; x, \tau')$  is relative to the electromagnetic field and  $K_D(\tau, \tau')$  relative to the detector and encoding its properties (bandwidth, efficiency etc). The first order correlation function defined

by Glauber<sup>4</sup> is defined as

$$\mathcal{G}_\rho^{(1)}(x, \tau; x', \tau') = \text{Tr}(E^{(+)}(x, \tau) \rho E^{(-)}(x', \tau')) \quad (2)$$

where  $E^{(+)}$  (resp.  $E^{(-)}$ ) respectively denote the annihilation and creation part of the electromagnetic field and  $\rho$  its density operator. Correlators involving a single time measure spatial coherence properties whereas taking all operators at the same position but various times gives a measurement of temporal coherence.

A broadband detector is characterized by  $K_D(\tau, \tau') \sim \delta(\tau - \tau')$ . In this case, the photodetection signal is directly proportional to the instantaneous photocount  $I(x, t) \sim \langle E^{(+)}(x, t) E^{(-)}(x, t) \rangle_\rho$  at the detector's position  $x$ . On the contrary, a narrow band detector will only retain the contribution of photons at a given frequency:  $K_D(\tau, \tau') \sim e^{i\Omega(\tau - \tau')}$ . Finally, Glauber defines higher order correlators which give the photodetection signals associated with the detection coincidences by several detectors<sup>4</sup>.

## B. Single electron coherence

The analogous of Glauber correlators for electrons propagating in a metallic system are electron and hole Keldysh correlation functions:

$$\mathcal{G}_\rho^{(e)}(x, t; y, t') = \text{Tr}(\psi(x, t) \rho \psi^\dagger(y, t')) \quad (3a)$$

$$\mathcal{G}_\rho^{(h)}(x, t; y, t') = \text{Tr}(\psi^\dagger(x, t) \rho \psi(y, t')). \quad (3b)$$

They describe the single-electron coherence considered in many-body approaches to the problem of electronic coherence in metals<sup>43,44</sup>. They are also directly related to detection signals since the tunneling current from the conductor to a reservoir contains two contributions arising from electron transmitted from the conductor to the reservoir and vice versa:

$$I_D(t) = \int_0^t \left( \mathcal{G}_\rho^{(e)}(x, \tau; x, \tau') K_a(\tau - \tau') - \mathcal{G}_\rho^{(h)}(x, \tau; x, \tau') K_e(\tau - \tau') \right) d\tau d\tau' \quad (4)$$

In this expression,  $K_a(\tau)$  and  $K_e(\tau)$  characterize the detector and respectively account for available single electron and hole states within the reservoir and for the eventual energy filtering of the detector. Let us stress that such a detection has been recently implemented experimentally to study electron relaxation in quantum Hall edge channels<sup>45</sup>.

The first important difference with usual quantum optics is the fact that ground state has a non vanishing single particle coherence whereas Glauber correlators vanish in the photon vacuum. On the contrary, at zero temperature, the single electron coherence within a single chiral channel is given by:

$$\mathcal{G}_\mu^{(e)}(x, y) = \frac{i}{2\pi} \frac{e^{ik_F(\mu)(x-y)}}{y - x + i0^+} \quad (5)$$

where  $k_F(\mu)$  denotes the Fermi momentum associated with the chemical potential  $\mu$  of the edge channel under consideration. At temperature  $T > 0$  K, these correlators decay over the thermal length scale  $l(T) = \hbar v_F / k_B T$  where  $v_F$  denotes the Fermi velocity.

It is then natural to decompose the single electron coherence in a Fermi sea contribution due to the chemical potential  $\mu$  of the conductor and a contribution due to electrons above this ground state:

$$\mathcal{G}^{(e)}(x, y) = \mathcal{G}_\mu^{(e)}(x, y) + \Delta \mathcal{G}^{(e)}(x, y) \quad (6)$$

The case of an ideal single electron excitation helps clarifying the physical meaning of  $\Delta \mathcal{G}^{(e)}$ . Such a state is obtained from a Fermi sea by adding one extra-particle in a normalized wave packet  $\varphi_0$ :

$$\psi^\dagger[\varphi_0]|F\rangle = \int_{-\infty}^{+\infty} \varphi_0(x) \psi^\dagger(x) |F\rangle \quad (7)$$

where  $|F\rangle$  denotes the Fermi sea at a fixed chemical potential. It is assumed that in momentum space,  $\varphi_0$  only has components on single particle states above the Fermi level. Then, Wick's theorem leads to

$$\Delta \mathcal{G}_{\psi^\dagger[\varphi_0]|F}^{(e)}(x, y) = \varphi_0(x) \varphi_0(y)^*. \quad (8)$$

In the same way, the single electron coherence of the state obtained by adding a single hole excitation to the Fermi sea  $\psi[\varphi_h]|F\rangle$  ( $\varphi_h(k) = 0$  below the Fermi level) is given by  $\Delta \mathcal{G}_{\psi[\varphi_h]|F}^{(e)}(x, y) = -\varphi_h(x) \varphi_h^*(y)$ . Note that the  $-$  sign reflects the fact that a hole is an absence of an electron from the Fermi sea. These simple examples show that  $\Delta \mathcal{G}^{(e)}$  contains all the information relative to the wavefunctions of excitations emitted by a single electron source.

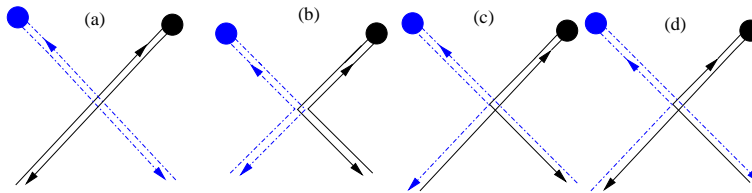


FIG. 1: Contributions to the probability of coincidence detection in quantum mechanics: the dashed (resp. full) lines corresponds to a single particle ending in the left (resp. right) detector represented here as filled blue (resp. black) dots. Each ascending arrows corresponds to a quantum amplitude associated with a single particle trajectory whereas a descending arrow corresponds to the complex conjugate of such an amplitude. Diagrams (a) and (b) thus represent classical two particle trajectories whereas (c) and (d) represent contributions of interferences between direct and exchange paths for two particle trajectories which are responsible for the HBT effect.

## II. QUANTUM TOMOGRAPHY

### A. Formulating the problem

An important issue of quantum optics is the characterization of the quantum state emitted by a source. Since photons are bosons, in the case of a monochromatic source, the problem is to reconstruct the quantum state of a single mode of the electromagnetic field. Spectacular results in quantum state preparation and measurement have recently been achieved in the microwave domain using cavity QED with Rydberg atoms<sup>46</sup> and superconducting nanocircuits (circuit QED)<sup>19</sup>.

On the contrary, in electron quantum optics, the Pauli exclusion principle prevents the emission of more than one electron in a single particle state. In this context, the question is to characterize the single particle excitations emitted by the source: this problem is called single electron tomography and consists in measuring the single electron coherence  $\Delta\mathcal{G}^{(e)}$ . This goes beyond the determination of the average current which only probes the diagonal of  $\Delta\mathcal{G}^{(e)}$  in the time domain. This also goes beyond measuring the electron distribution number since this quantity characterizes single electron coherence only in a stationary situation but not in the case of a pulsed single electron source.

### B. The Hanbury Brown & Twiss effect

In quantum optics, quantum tomography can indeed be achieved using two particle quantum interferences<sup>47,48</sup>. The idea is to rely on the Hanbury Brown Twiss (HBT) effect which consists in intensity correlations and anti-correlations in a coherent scattering experiment involving two incoming beams of identical quantum particles. Whereas natural in classical electromagnetism, the effect was somehow disputed in the optical domain. The controversy stopped with the demonstration of the effect in the laboratory<sup>2,49</sup> after it was used to measure the diameter of stars within the principal sequence<sup>1</sup>. Later, Fano provided the proper quantum interpretation in term of two photon interferences<sup>50</sup>. Since its discovery, the HBT effect has also been observed for electrons in a metal issued by two different reservoirs at equilibrium<sup>51-53</sup>. It has also been used in nuclear physics where it provides information on the space time geometry of particle pair production regions in heavy ion collisions<sup>54</sup>. More recently, a beautiful experiment conducted with metastable Helium atoms demonstrated the effect for fermionic (<sup>3</sup>He) and bosonic (<sup>4</sup>He) atoms which exhibited the bunching and antibunching behavior expected from their quantum statistics<sup>55</sup>.

To understand the effect, imagine that we observe a coincidence between two detectors  $A$  and  $B$  observing an ensemble of sources, each of them emitting a single particle for simplicity. Figure 1 depicts the various contributions to such a coincidence event. Two of them can be interpreted in terms of classical trajectories where a particle emitted by a given source is detected by a given detector. But for indistinguishable quantum particles, the coincidence probability involves interferences between two particle paths which differ by exchange. These are thus sensitive to the particle's quantum statistics.

Now if we imagine having single particle sources, the HBT effect will occur if and only if both sources emit particles in the same quantum state and in a synchronized way otherwise they could be distinguished<sup>56</sup>. This has been observed for two photons emitted by a non linear cristal by Hong, Ou and Mandel (HOM)<sup>57</sup> and 20 years later for photons emitted by two independent sources<sup>58</sup>.

This strongly suggests that a controlled source could be used to characterize the single particle content of an unknown source using the HBT interferometry setup depicted on Figure 2. This idea has been exploited to perform

the quantum tomography of a single mode of the electromagnetic field using a laser as the known source, called a local oscillator<sup>47</sup>. But in the context of electron quantum optics, Fermi statistics forbids the existence of classical wave and thus of a laser. For single electron tomography, we need a controlled and characterized source able to sweep the space of single particle states. An ohmic contact provides this appropriate local oscillator since its chemical potential can be varied to scan the relevant energy range of single electron and hole excitations emitted by the source to be characterized.

### C. Single electron quantum tomography

The Hanbury Brown & Twiss (HBT) setup depicted on figure 2 is designed to perform the analogous of homodyne tomography in quantum optics. A quantum point contact (QPC) playing the role of a beam splitter for electrons. The source to be characterized is placed on the incoming channel 1 whereas an Ohmic contact with controlled time dependent chemical potential  $\mu_2(t) = \mu_2 - eV_{ac}(t)$  is placed on incoming channel 2. We measure current correlations between the two outgoing channels. Time dependent correlations are defined as:

$$S_{\alpha\beta}^{\text{out}}(t, t') = \langle i_{\alpha}^{\text{out}}(t) i_{\beta}^{\text{out}}(t') \rangle - \langle i_{\alpha}^{\text{out}}(t) \rangle \langle i_{\beta}^{\text{out}}(t') \rangle. \quad (9)$$

The outgoing current correlations can be expressed in terms of the incoming ones  $S_{\alpha\beta}^{\text{in}}(t, t')$  and of a contribution  $\mathcal{Q}(t, t')$  coming from two particle interferences. This HBT contribution  $\mathcal{Q}(t, t')$  involves the incoming single particle coherences right upstream the QPC:

$$\mathcal{Q}(t, t') = (ev_F)^2 \left( \mathcal{G}_1^{(e)} \mathcal{G}_2^{(h)} + \mathcal{G}_2^{(e)} \mathcal{G}_1^{(h)} \right) (t', t) \quad (10)$$

and the final expressions for outgoing current correlations are

$$S_{11}^{\text{out}}(t, t') = \mathcal{R}^2 S_{11}^{\text{in}}(t, t') + \mathcal{T}^2 S_{22}^{\text{in}}(t, t') + \mathcal{R}\mathcal{T} \mathcal{Q}(t, t') \quad (11)$$

$$S_{22}^{\text{out}}(t, t') = \mathcal{T}^2 S_{11}^{\text{in}}(t, t') + \mathcal{R}^2 S_{22}^{\text{in}}(t, t') + \mathcal{R}\mathcal{T} \mathcal{Q}(t, t') \quad (12)$$

$$S_{12}^{\text{out}}(t, t') = S_{21}^{\text{out}}(t, t') = \mathcal{R}\mathcal{T} (S_{11}^{\text{in}}(t, t') + S_{22}^{\text{in}}(t, t') - \mathcal{Q}(t, t')) \quad (13)$$

where  $\mathcal{R}$  and  $\mathcal{T}$  are the reflexion and transmission probabilities of the QPC. Equation (10) shows that the HBT contribution is of truly quantum origin: it vanishes when the time separation is larger than the quantum coherence time within the two incoming channels. Outgoing correlations are then caused by classical partitioning of current fluctuations at the QPC. To perform single electron quantum tomography we reconstruct  $\Delta\mathcal{G}_1^{(e)}$  for the unknown source using (10) by studying the variation of the HBT contribution when parameters of the controlled source on channel 2 are varied.

The quantum tomography protocols relies on the measurement of the time averaged low frequency component of current correlations:

$$S_{\alpha\beta}^{\text{exp}} = \int \overline{S_{\alpha\beta}^{\text{out}}(\bar{t} + \tau/2, \bar{t} - \tau/2)}^{\bar{t}} d\tau \quad (14)$$

But then, a stationary source on channel 2 can only give access to the stationary part of  $\Delta\mathcal{G}_1^{(e)}$  since one measures time averaged quantities. Applying a periodic voltage to the ohmic contact at frequencies corresponding to the harmonics of the driving frequency of the source precisely performs the homodyning needed to capture the  $\bar{t} = (t+t')/2$  dependence of  $\Delta\mathcal{G}_1^{(e)}$ . Details of the tomography protocol are given in our recent work<sup>59</sup>. Let us just recall that the output of our tomography protocol is the single particle coherence  $\Delta\mathcal{G}_1^{(e)}$  in the frequency domain since current correlations themselves are measured in the frequency domain.

To support the feasibility of this tomography protocol, we have made explicit predictions for the single electron coherence and for the correlation signals expected for an on demand single electron source<sup>59</sup>. These predictions, obtained within the framework of Floquet scattering theory, shed light on the various regimes of the source and on its potential performances. They also give estimates of noise sensitivity required to perform the experiment:  $10^{-30}$  A<sup>2</sup>/Hz. Such a resolution is within reach of ultrahigh sensitivity noise measurement techniques<sup>40,41</sup>.

To conclude this section, let us stress that other experiments based on the HBT interferometer have been proposed such as noise measurements in an HOM setup<sup>60</sup> and spectroscopy of electron flows<sup>61</sup>. Finally, a recent proposal aims at producing orbitally entangled pairs of electrons by combining an HBT interferometer with two Mach-Zehnder interferometers<sup>62</sup>. We thus hope that experimental groups will soon be able to demonstrate experiments combining an HBT interferometer with single electron sources.

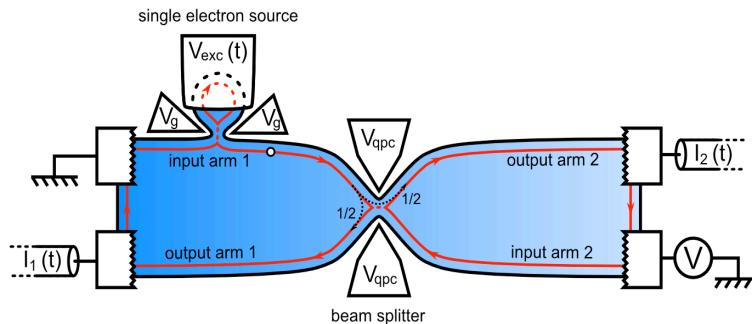


FIG. 2: Hanbury Brown & Twiss setup for single electron tomography: This setup is designed to characterize the single electron coherence of an on demand single electron source present on the incoming branch 1 close to the QPC (here  $\mu_1 = 0$ ) and driven by the voltage  $V_{\text{exc}}(t)$ . A reservoir with a time dependent chemical potential  $\mu_2(t) = -eV(t) = \mu_2 - eV_{\text{ac}}(t)$  is connected to the incoming branch 2. One measures the low frequency correlation  $S_{12}^{\text{exp}}$  of the outgoing current  $I_1$  and  $I_2$ .

### III. ELECTRON DECOHERENCE AND RELAXATION

Mach-Zehnder interferometry experiments have demonstrated single electron coherence in quantum Hall edge channels but have also drew attention on electron decoherence and its mechanisms. In particular, at filling fraction  $\nu = 2$ , experimental studies have shown that inter-channel Coulomb interactions are the main source of decoherence for electrons propagating within one edge channel<sup>63–65</sup>. Recent experimental studies of electron relaxation<sup>45,66,67</sup> have also shown that in this system, single electron excitations are ill defined and this suggests that screened inter-channel Coulomb interactions cannot be considered as weak.

The aforementioned experiments are quantum transport experiments involving non equilibrium distribution functions. But with the demonstration of a single electron source, the problem of quasiparticle relaxation (and decoherence) originally considered by Landau in Fermi liquid theory<sup>68</sup> could be tested experimentally within quantum Hall edge channels in the near future. This single quasiparticle relaxation problem is simpler than the relaxation of a general stationary non equilibrium electronic state but nevertheless is conceptually important since it probes the nature of quasiparticle in quantum Hall edge channels and questions the validity of the quantum optics paradigm in these systems.

To address this problem, a unified approach to high frequency transport and to decoherence and relaxation of single electron excitations has been developed<sup>69,70</sup>. In this approach, we consider their propagation across an interaction region where possibly strong Coulomb interactions are present or which is capacitively coupled to an external conductor or circuit behaving as an harmonic environment as shown on figure 3.

#### A. Interactions and high frequency transport

Bosonization essentially describes chiral 1D systems in terms of free bosonic modes, called edge magnetoplasmons, that describe electron/hole excitations above a Fermi sea vacuum. Within the bosonization formalism, electron/electron interactions as well as capacitive coupling to a linear environment lead to a quadratic Hamiltonian in the bosonic field describing the bosonized edge channel and the environmental modes. The equations of motion can thus be solved exactly and, in the geometry of figure 3, it leads to a scattering matrix describing the elastic scattering between edge magnetoplasmons and environmental modes. All the dynamics is encoded into the frequency dependence of the transmission and reflexion coefficients.

Although the plasmon scattering matrix seems to be a rather abstract object, it turns out to be directly related to finite frequency admittances which are measurable quantities. Such an idea was pioneered within the context of non chiral 1D Luttinger liquid by Safi and Schulz<sup>71,72</sup> in the mid-90s. Let us consider a chiral system involving several edge channels electrostatically interacting within an interaction region of length  $l$ . Each of these channels  $\alpha$  is attached to an Ohmic contact driven by a time dependent voltage  $V_\alpha(t)$  generating a coherent magnetoplasmon state. Within the bosonization formalism, the interaction region acts as frequency dependent beam splitter for edge magnetoplasmons. The incoming coherent states are then scattered into outgoing coherent states whose amplitudes are given in terms of the incoming ones by the plasmon scattering matrix, exactly like for classical waves scattered by a beam splitter in classical electromagnetism. Using the expression of edge currents in terms of the magnetoplasmon modes, one

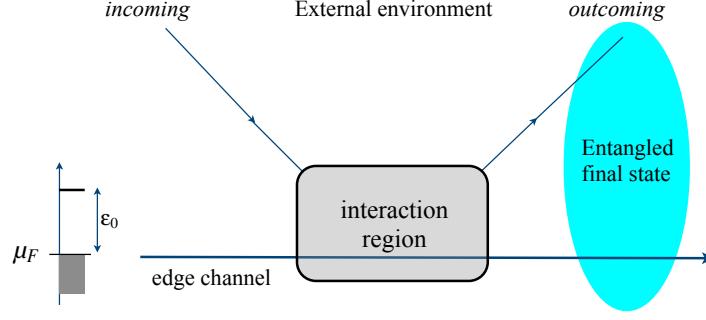


FIG. 3: Scattering approach to decoherence and relaxation in quantum Hall edge channels: an incoming state is injected from the left into an interaction region in which edge magnetoplasmons and environmental modes are elastically scattered. This leads to an entangled state between the edge channel and environmental degrees of freedom. We then evaluate the outcoming single electron coherence:  $\Delta\mathcal{G}_{\text{out}}^{(e)}(x, y)$ .

immediately obtains a linear relation between the average time dependent currents  $I_\alpha$  entering the interacting region of each edge channel in terms of the voltage applied to the Ohmic reservoirs:

$$I_\alpha(\omega) = \frac{e^2}{h} \sum_{\beta} g_{\alpha\beta}(\omega) V_\beta(\omega). \quad (15)$$

The important point is that the finite frequency dimensionless admittance matrix  $g_{\alpha\beta}(\omega)$  is given in terms of the plasmon scattering matrix  $S_{\alpha\beta}(\omega)$  relating incoming to outgoing plasmonic modes:

$$g_{\alpha\beta}(\omega) = \delta_{\alpha\beta} - S_{\alpha\beta}(\omega). \quad (16)$$

For example, in the case of free propagation along a single edge channel with time of flight  $\tau$ ,  $S(\omega) = e^{i\omega\tau}$  and therefore  $g(\omega) = 1 - e^{i\omega\tau}$ . For an edge channel  $\alpha$ , the relation  $g_{\alpha\alpha}(\omega) = 1 - S_{\alpha\alpha}(\omega)$  is indeed true even in the presence of an external electromagnetic environment, provided  $S_{\alpha\alpha}(\omega)$  denotes the edge magnetoplasmon transmission amplitude taking into account scattering into environmental degrees of freedom. Of course, for a given circuit design, this quantity is model dependent since it requires an explicit description of Coulomb interactions and screening effects. Nevertheless, in the limit where the frequency is low compared to the inverse of the longest time of flight across the system, a discrete element approach developed by Büttiker and his collaborators<sup>73,74</sup> can be used. In this regime, the low frequency expansion of this finite frequency admittance  $g(\omega)$  is generically of the form

$$g(\omega) = -iR_K C_\mu \omega + \frac{R_q}{R_K} (R_K C_\mu \omega)^2 + \text{higher orders}. \quad (17)$$

where  $C_\mu$  denotes the electrochemical capacitance and  $R_q$  the relaxation resistance of the conductor formed by the interaction region coupled to its environment. As shown by Büttiker, Prêtre and Thomas<sup>73,74</sup>, the relaxation resistance  $R_q$  is the serial addition of the edge channel relaxation resistance  $R_K/2$  and of the environmental resistance  $R$ . The latter is related to the density of states available for dissipation in the electromagnetic environment of the edge channel. The  $R_K/2$  value is robust to interactions within the quantum capacitor's plate<sup>75,76</sup>. It indeed reflects the presence of a single mode coherent conductor connected to free electron reservoirs since  $R_q$  is renormalized in the fractional quantum Hall regime<sup>77</sup> and is equal to the classical result in the presence of strong decoherence effects within the capacitor<sup>78</sup>. The electrochemical capacitance is also the series addition of its quantum capacitance associated with the dot density of states and of the geometric capacitance between the edge channel and its environment. In the case of free propagation, expanding  $g(\omega) = 1 - e^{i\omega\tau}$  in powers of  $\omega$  and comparing to (17) shows that  $R_K C_\mu$  is nothing but the electron time of flight  $\tau$  as noticed by Imry and his collaborators<sup>79</sup>.

The Büttiker, Prêtre and Thomas predictions have been experimentally tested for the quantum RC circuit<sup>80</sup> and also for the quantum RL circuit<sup>81</sup>. As will become clear in the forthcoming section, the availability of admittance measurements in the GHz frequency range opens exciting perspectives for quantitative tests of the plasmon scattering approach to single electron relaxation within quantum Hall edge channels.

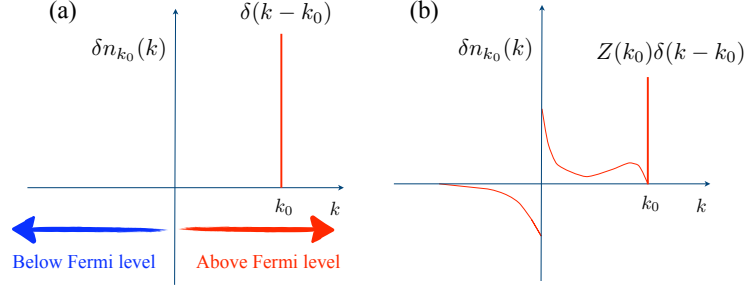


FIG. 4: (a) Incoming single electron coherence for an initial energy resolved single electron excitation above the Fermi level. (b) Outcoming single electron coherence  $\delta n_{k_0}(k)$ : at  $k = k_0$ , the quasiparticle peak comes is the contribution of electrons flying across the interaction region without losing energy (elastic scattering probability).

### B. Quasiparticle relaxation in quantum Hall edge channels

The problem considered by Landau to lay the foundations of Fermi liquid theory<sup>68</sup> is to determine how a single electron excitation of given energy introduced in an interacting electronic system relaxes. In the geometry of figure 3, one would consider an incoming single electron excitation of momentum  $k_0 > 0$  and ask what would be the single electron coherence coming out from the interaction region. Because an energy resolved single electron excitation can be described as a superposition of coherent states of edge magnetoplasmons, this problem can be solved exactly. The result is a non perturbative solution of the Landau quasiparticle relaxation problem in quantum Hall edge channels<sup>69</sup>.

At zero temperature, the final result is expected to be of the form depicted on figure 4: the incoming electron distribution function  $\delta n_{k_0}^{(\text{in})}(k) = \delta(k - k_0)$  comes out of the interacting region as  $\delta n_{k_0}^{(\text{out})}(k) = Z(k_0)\delta(k - k_0) + \delta n_{k_0}^r(k)$  where  $0 \leq Z(k_0) \leq 1$  represent the probability for the incoming electron to be scattered elastically and  $\delta n_{k_0}^r(k)$  is a regular function, representing the energy relaxation of the incoming electron. Particle conservation implies the sum rule  $\int \delta n_{k_0}^{(\text{out})}(k) dk = 1$ . Note that  $\delta n_{k_0}^r(k) = 0$  for  $k > k_0$  and  $k < -k_0$  since we are at zero temperature (no heating) and the available energy from the incoming electron is at most  $\varepsilon_0 = \hbar v_F k_0$ .

Our main results<sup>69</sup> are non perturbative analytical expressions for  $Z(k_0)$  and  $\delta n_{k_0}^r(k)$  which only depend on the finite frequency admittance  $g(\omega)$ . As expected, for  $g(\omega) = 1 - e^{i\omega\tau}$  (free electron propagation)  $Z(k_0) = 1$  and  $\delta n_{k_0}^r(k) = 0$  meaning that the electron does not relax at all. When interactions are present, it is interesting to discuss the full non perturbative results in the limit of very low energy to test the validity of the Fermi liquid paradigm and, in the limit of increasing energy, to discuss the validity of the quantum optics paradigm for electronic flying qubits<sup>82</sup>.

At low energy, the Pauli principle blocks inelastic processes and the elastic scattering probability  $Z(k_0) \rightarrow 1$  when  $k_0$  decays to zero. Using the low frequency expansion of the finite frequency admittance (17), the low energy behavior of the inelastic scattering probability  $\sigma_{\text{in}}(\varepsilon_0) = 1 - Z(\varepsilon_0/\hbar v_F)$  can be obtained as:

$$\sigma_{\text{in}}(\varepsilon_0) = \left( \frac{R_q}{R_K} - \frac{1}{2} \right) (\varepsilon_0 R_K C_\mu / \hbar)^2 + \text{higher orders}. \quad (18)$$

The dominant term represents energy losses into the external environment and has a simple universal form. Since the inelastic probability scales at least as  $\varepsilon_0^2$ , the quasiparticle is preserved in the limit of very low energies as expected in a Fermi liquid. The case  $R = 0$  describes the coupling to a perfectly conducting top gate beneath which electrons within the chiral edge channel experience long range Coulomb interactions. In this case, at low frequency,  $\sigma_{\text{in}}(\varepsilon_0)$  starts with a higher power:

$$\sigma_{\text{in}}(\varepsilon_0) = \frac{11}{25920} \left( \frac{C_\mu}{C - C_\mu} \right)^2 (\varepsilon_0 R_K C_\mu / \hbar)^6 + \text{higher orders}. \quad (19)$$

This behavior is not universal since it still depends on the geometrical capacitance  $C$  coupling the edge channel to the top metallic gate and not only on the electrochemical capacitance  $C_\mu$  and the relaxation resistance  $R_K/2$  which describe the response properties of the quantum RC circuit formed by the interaction region capacitively coupled to a perfectly conducting top gate. Figure 5 summarizes these results by depicting the exact elastic probability<sup>69</sup>  $Z(\varepsilon_0)$  and their low energy behaviors given by eqs. (18) and (19). Finally, we would like to point out that tailoring



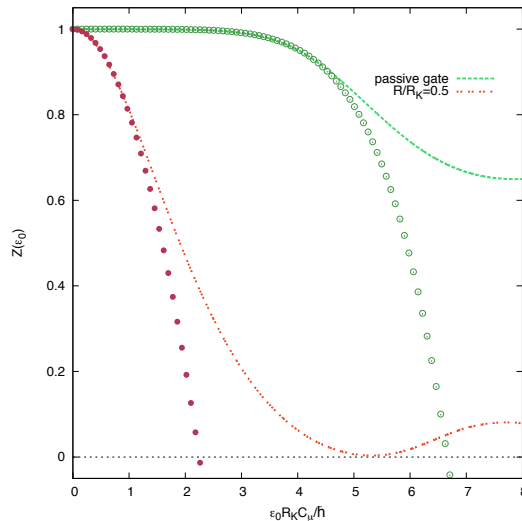


FIG. 5: Elastic scattering probability  $Z(\varepsilon_0)$  as a function of  $\varepsilon_0 R_K C_\mu / \hbar$  in the case of the quantum RC circuit for  $R = R_K/2$  (dot-dashed line) and  $R = 0$  (dashed line) and low energy behaviors given by eqs. (18) and (19) (circular dots).

properly the electrostatic neighborhood of the edge channel so that it doesn't lead to energy leaks leads to decoherence shielding for single electron excitations at least at low enough energy. The validity of this idea has been experimentally demonstrated by F. Pierre and his collaborators<sup>67</sup>.

At higher energies, two scenarii are possible. At low coupling, that is when  $g(\omega)$  does not depart too much from a free electron behavior, the extra electron relaxes but can still be distinguished by its energy from electron/hole pairs generated within the Fermi sea as illustrated on figure 4b. Then, the Fermi sea can be viewed as an extra dissipation channel. In this case, the single electron wavepacket decoheres according to

$$\varphi(x) \varphi(y)^* \mapsto \mathcal{D}(x-y) \varphi(x) \varphi(y)^* \quad (20)$$

where  $\mathcal{D}(x-y)$  is an effective decoherence coefficient representing the action of an effective environment on the quasi particle going through the interaction region. Its expression in terms of the finite frequency admittance is similar to the one obtained in the dynamical Coulomb blockade theory<sup>33–35</sup>:

$$\mathcal{D}(x-y) = \exp \left( \int_0^{+\infty} \Re(g(\omega)) (e^{-i\omega(x-y)/v_F} - 1) \frac{d\omega}{\omega} \right). \quad (21)$$

But at stronger coupling and high enough energy, this description breaks down. In this case, it is no longer possible to distinguish between the incoming extra electron and electrons stemming from electron/hole pairs excitations created within the Fermi sea by Coulomb interactions. A typical situation where this happens is the case of quantum Hall edges at filling fraction  $\nu = 2$  which involves two copropagating spin polarized channels coupled through Coulomb interactions.

### C. Energy relaxation in $\nu = 2$ systems

Recently, F. Pierre and his collaborators have studied energy relaxation in quantum Hall edge channels at  $\nu = 2$ . Using a quantum dot as a spectrometer, they have measured the electron distribution function in one of the two edge channels<sup>45</sup>. Their experimental setup has been designed to study the relaxation of a non equilibrium distribution function generated by a biased quantum point contact after propagation over several lengths ranging from  $l = 0.8 \mu\text{m}$  to  $l = 30 \mu\text{m}$ . Experimental data<sup>66,67</sup> show that inter-channel interaction is responsible for the energy relaxation in this system and arises from Coulomb interactions that are screened by metallic gates shaping the 2DEG (see Figure 1 of<sup>66</sup>). Therefore, this experiment could be used to test the plasmon scattering approach to interacting quantum Hall edge channels.

In a recent work<sup>70</sup>, we have studied the simplest model describing a system of two copropagating quantum Hall edge channels. We have shown, that under physically reasonable assumptions, the plasmon scattering matrix had

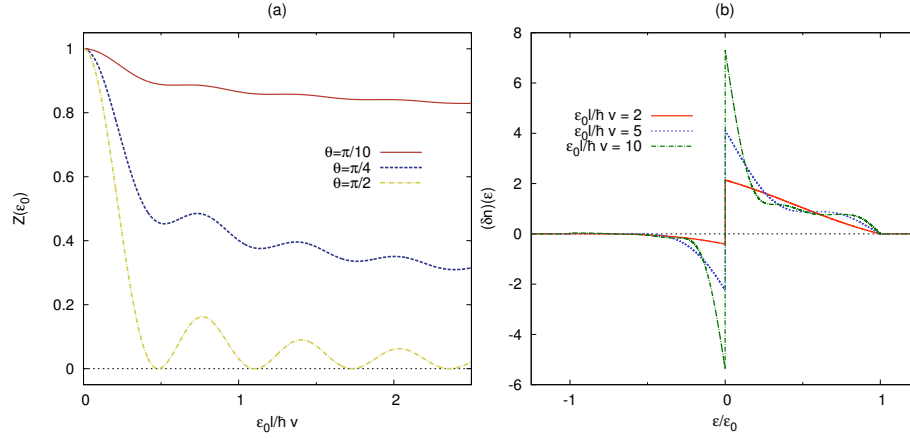


FIG. 6: Relaxation in the two channel system: (a)  $Z(\varepsilon_0)$  as a function of  $\varepsilon_0 l / \hbar v$  for weak to strong coupling:  $\theta = \pi/10$  (full line),  $\theta = \pi/4$  (dashed line),  $\theta = \pi/2$  (long dashed line). (b)  $\delta n_{\varepsilon_0}^r(\varepsilon)$  as a function of  $\varepsilon / \varepsilon_0$  at strong coupling ( $\theta = \pi/2$ ) for various propagation lengths.

a universal form at low energy. This  $2 \times 2$  unitary matrix  $S(\omega, l)$  corresponding to the scattering by an interacting region of length  $l$  is of the form

$$S(\omega, l) = e^{i\omega l / v_0} e^{-i(\omega l / v)(\cos(\theta)\sigma^z + \sin(\theta)\sigma^x)} \quad (22)$$

where  $v_{\pm}^{-1} = v_0^{-1} \mp v^{-1}$  are the velocities of the true eigenmodes of the coupled edge channel system which are linear combinations, characterized by the angle  $\theta$ , of the edge magnetoplasmon modes of the two channels. Strongly coupled edge channels correspond to  $\theta = \pi/2$ , a situation already considered in the recent theoretical study of MZI at  $\nu = 2$  by Levkivsky and Sukhorukov<sup>83</sup>. Then, the eigenmodes of the coupled system correspond to charge and spin density waves, the latter being the slowest of the two.

Using the scattering matrix (22), the relaxation of single electron excitations can be computed. At strong coupling ( $\theta = \pi/2$ ),  $Z(\varepsilon_0) = (J_0(\varepsilon_0 l / \hbar v))^2$  showing that the quasi particle decays after propagation over  $l_{\text{in}} \simeq \hbar v / \varepsilon_0$ , consistent with the semi-quantitative conclusion from the experimental group<sup>66</sup>. Figure 6a presents the decay of  $Z(\varepsilon_0)$  for various values of  $\theta$ , showing that  $\theta = \pi/2$  leads to the fastest decay and that, for  $\theta \ll \pi/2$  (weak coupling), the quasi particle propagates over a much longer distance. Looking at the complete electronic relaxation for  $\theta = \pi/2$  depicted on figure 6b shows that, once the quasi particle peak has decayed, the incident electron has been drawn into the electron/hole pairs it has generated. Thus, although for a fixed  $l$ , the notion of a quasi particle in this  $\nu = 2$  edge channel system makes sense at low energy ( $\varepsilon_0 \ll \hbar v / l$ ), it cannot be viewed as a Fermi liquid in the thermodynamic limit since a quasi particle of given energy will disappear after propagation over  $l_{\text{in}}(\varepsilon_0) \simeq \hbar v / \varepsilon_0$ , meaning that its energy width is proportional to its energy. At high energies, relaxation of single electron excitations cannot be described within a simple dynamical Coulomb blockade picture and electronic quasi particles are ill defined.

Although computing the exact relaxation of the electron distribution function is a complicated task, it is much simpler to compute the evolution of heat currents along each edge channel since it only requires two point functions of the current injected by the biased QPC. These predictions can then be compared to the experimental data<sup>70</sup>. We have shown that using a typical value for the velocity  $v \simeq 10^5 \text{ ms}^{-1}$ , the two channel model reproduces correctly the dependence of the heat current in the QPC bias voltage and length assuming ad hoc 25 % of the energy leaks out. This leaking was interpreted as a manifestation of extra degrees of freedom such as neutral modes arising from the eventual compressibility of the inner edge channel.

Note that an alternative approach based on the Boltzmann equation has been developed by Lunde, Nigg and Büttiker<sup>84</sup> which also fits the experimental data at the price of assuming also an energy leak towards other degrees of freedom. Finally, in their recent work<sup>85</sup>, Kovrizhin and Chalker have suggested that the effective temperature deduced from tunneling measurements differs from the effective temperature representing the real heat current due to an interaction induced renormalization of the tunneling density of state.

At this point, it should be noticed that the total heat current being an integrated quantity, it does not give an energy resolved information. The electron distribution function does give access to such an information but the issue of the tunneling DOS as well as the difficulty to perform predictive computations for this quantity implies that it may not be the best quantity to confront theoretical models to experimental data. Within the plasmon scattering approach, finite frequency current noise directly provides a frequency resolved information on the population of the

edge magnetoplasmon modes. This is why we have suggested to use such measurement as well as finite admittance measurements to probe edge magnetoplasmon scattering<sup>70</sup>.

As shown by the flurry of theory papers devoted to the discussion of electron dephasing<sup>86,87</sup> and fringe visibility<sup>65,88–94</sup>, the Mach-Zehnder interferometer would deserve a full review by itself. We would just like to point out that although  $Z(k_0)$  naturally appears as the contrast reduction of interference fringes for energy resolved single electrons sent into a Mach-Zehnder interferometer, Levkivskyi and Sukhorukov<sup>83</sup> have shown that understanding MZI experiments involving electron flows from reservoirs also requires, beside decoherence effects, to properly consider electrochemical potential shifts within the interferometer, a point also stressed by Roche *et al*<sup>64</sup>. Moreover new phenomena have been predicted: when a non equilibrium Fermi double step electron distribution function is injected into an incoming channel of the interferometer, non Gaussian fluctuations of the current can induce a quantum phase transition on the lobe structure of the visibility<sup>95</sup>.

#### IV. CONCLUSION AND PERSPECTIVES

Recent progresses in nanofabrication and radiofrequency technology and in ultrahigh sensitivity noise measurements have opened the way to new experiments aiming at the controlled manipulation of elementary excitations in ballistic quantum conductors similar to what is done with photons in quantum optics. These experiments have already stimulated an important stream of theoretical research on the formulation of “electron quantum optics” taking into account interactions and discussing the dynamics of single to few electron excitations in the presence of interactions.

The main message we would like to pass to the reader is that the emerging field of electron quantum optics really provides a radically new point of view on quantum transport and more generally on mesoscopic physics.

First of all, electron quantum optics really concerns the exploration of time scales comparable to the characteristic times of electron dynamics within quantum conductors, *i.e.* the time of flight and the decoherence time which are of the order of tens to hundreds of picoseconds. Next, instead of dealing with non-equilibrium many body states involving a large number of electrons, electron quantum optics deals with one to few elementary excitations, a situation conceptually much simpler than in a far from equilibrium quantum transport experiment. Interestingly the recently developed non equilibrium bosonization<sup>96,97</sup> should provide the technical basis for understanding the role of non Gaussian fluctuations in single electron devices and also for understanding the close relation between electron quantum optics and full counting statistics<sup>98</sup>.

Moreover, on the experimental side, electron quantum optics clearly requires a new way of doing mesoscopic physics by bringing new tools to prepare, control and record quantum states. On the conceptual side, it brings in concepts from quantum information theory such as entanglement, fidelities and entanglement entropies.

Finally, although analogies with quantum optics should be stressed, a rich physics emerges from differences between photons and electrons: understanding the interplay of Coulomb interactions and of the Fermi statistics in a mesoscopic conductor is a highly non trivial problem which has already attracted a lot of attention<sup>44,99</sup>. It touches deep questions such as the nature and dynamics of quasiparticles in mesoscopic conductors. Electron quantum optics can bring new insights on these important issues since we can now envision *gedanken experiment* never realized before such as controlled decoherence experiments involving single to few electron excitations by exploiting controlled couplings to external circuits. Our highest hopes are therefore within the hands of experimentalists. The successful demonstration of new electron quantum optics experiments such as single electron tomography will really mark the beginning of a new era.

#### Acknowledgments

We would like to thank C. Altimiras, M. Albert, J.M. Berroir, E. Bocquillon, M. Büttiker, Ch. Flindt, Ch. Glattli, Th. Jonckheere, H. Le Sueur, I. Levkivskyi, Th. Martin, S. Nigg, F. Pierre, F. Parmentier, B. Plaçais, F. Portier, J.M. Raimond, J. Rech, P. Roche, P. Rouleau and E. Sukhorukov for useful discussions.

---

<sup>1</sup> R. Hanbury Brown and R. Twiss, *Nature* **178**, p. 1046 (1956).

<sup>2</sup> R. Hanbury Brown and R. Twiss, *Nature* **177**, p. 27 (1956).

<sup>3</sup> R. Glauber, *Phys. Rev. Lett.* **10**, p. 84 (1962).

- <sup>4</sup> R. Glauber, *Phys. Rev.* **130**, p. 2529 (1963).
- <sup>5</sup> R. Glauber, *Phys. Rev.* **131**, p. 2766 (1963).
- <sup>6</sup> H. J. Kimble, M. Dagenais and L. Mandel, *Phys. Rev. Lett.* **39**, p. 691 (1977).
- <sup>7</sup> C. Hong and L. Mandel, *Phys. Rev. Lett.* **56**, p. 58 (1986).
- <sup>8</sup> P. Grangier, G. Roger and A. Aspect, *Europhys. Lett.* **1**, p. 173 (1986).
- <sup>9</sup> B. Lounis and M. Orrit, *Rep. Prog. Phys.* **68**, p. 1129 (2005).
- <sup>10</sup> C. Brunel, B. Lounis, P. Tamarat and M. Orrit, *Phys. Rev. Lett.* **83**, 2722 (1999).
- <sup>11</sup> A. Beveratos, R. Brouri, T. Gacoin, A. Villing, J.-P. Poizat and P. Grangier, *Phys. Rev. Lett.* **89**, p. 187901 (2002).
- <sup>12</sup> J. Kim, O. Benson, H. Kan and Y. Yamamoto, *Nature* **397**, p. 500 (1999).
- <sup>13</sup> M. Pelton, C. Santori, J. Vuckovic, B. Zhang, G. Solomon, J. Plant and Y. Yamamoto, *Phys. Rev. Lett.* **89**, p. 233602 (2002).
- <sup>14</sup> T. Yamamoto, M. Koashi, S. Özdemir and N. Imoto, *Nature* **421**, p. 343 (2003).
- <sup>15</sup> A. Kuzmich, W. Bowen, A. Doozer, A. Boca, C. Chou, L.-M. Duan and H. Kimble, *Nature* **423**, p. 721 (2003).
- <sup>16</sup> P. Kok, W. J. Munro, K. Nemoto, T. C. Ralph, J. Dowling and G. Milburn, *Rev. Mod. Phys.* **79**, 135 (2007).
- <sup>17</sup> S. Haroche and J.-M. Raimond, *Exploring the quantum* (Oxford University Press, 2006).
- <sup>18</sup> A. Blais, R.-S. Huang, A. Wallraff, S. Girvin and R. Schoelkopf, *Phys. Rev. A* **69**, p. 062320 (2004).
- <sup>19</sup> M. Hofheinz, H. Wang, M. Ansmann, R. Bialczak, E. Lucero, M. Neeley, A. O'Connell, D. Sank, J. Wenner, J. Martinis and A. Cleland, *Nature* **459**, p. 546 (2009).
- <sup>20</sup> Y. Ji, Y. Chung, D. Sprinzak, M. Heiblum, D. Mahalu and H. Shtrikman, *Nature* **422**, p. 415 (2003).
- <sup>21</sup> P. Roulleau, F. Portier, D.C. Glattli, P. Roche, A. Cavanna, G. Faini, U. Gennser and D. Mailly, *Phys. Rev. Lett.* **100**, p. 126802 (2008).
- <sup>22</sup> G. Lesovik, *JETP Letters* **49**, p. 592 (1989).
- <sup>23</sup> M. Büttiker, *Phys. Rev. Lett.* **65**, 2901 (1990).
- <sup>24</sup> T. Martin and R. Landauer, *Phys. Rev. B* **45**, 1742 (1992).
- <sup>25</sup> M. Büttiker, *Phys. Rev. B* **46**, 12485 (1992).
- <sup>26</sup> W. Schottky, *Ann. Phys. (Leipzig)* **57**, p. 1918 (1918).
- <sup>27</sup> P. Samuelsson, E. Sukhorukov and M. Büttiker, *Phys. Rev. Lett.* **92**, p. 026805 (2004).
- <sup>28</sup> I. Neder, N. Ofek, Y. Chung, M. Heiblum, D. Mahalu and V. Umansky, *Nature* **448**, p. 333 (2007).
- <sup>29</sup> E. Zakka-Bajjani, J. Segala, F. Portier, P. Roche, D.C. Glattli, A. Cavanna and Y. Jin, *Phys. Rev. Lett.* **99**, p. 236803 (2007).
- <sup>30</sup> G. Fève, A. Mahé, J.-M. Berroir, T. Kontos, B. Plaças, D.C. Glattli, A. Cavanna, B. Etienne and Y. Jin, *Science* **316**, p. 1169 (2007).
- <sup>31</sup> A. Mahé, F.D. Parmentier, E. Bocquillon, J.-M. Berroir, D.C. Glattli, T. Kontos, B. Plaças, G. Fève, A. Cavanna and Y. Jin, *Phys. Rev. B* **82**, p. 201309 (2010).
- <sup>32</sup> C. Beenakker, Electron-hole entanglement in the fermi sea, in *Quantum computers, Algorithms and Chaos*, eds. G. Casati, D. Shepelyansky, P. Zoller and G. Benenti, International School of Physics Enrico Fermi, Vol. 162 (IOS Press, Amsterdam, 2006).
- <sup>33</sup> M. Devoret, D. Esteve, H. Grabert, G.-L. Ingold, H. Pothier and C. Urbina, *Phys. Rev. Lett.* **64**, p. 1824 (1990).
- <sup>34</sup> S. Girvin, L. Glazman, M. Jonson, D. Penn and M. Stiles, *Phys. Rev. Lett.* **64**, p. 3183 (1990).
- <sup>35</sup> G.-L. Ingold and Y. Nazarov, *Single charge tunneling*, NATO ASI Series B Vol. 294 (Plenum Press, New York, 1992), ch. Charge tunneling rates in ultrasmall junctions, pp. 21–107.
- <sup>36</sup> B. Halperin, *Phys. Rev. B* **25**, 2185 (1982).
- <sup>37</sup> M. Büttiker, *Phys. Rev. B* **38**, p. 9375 (1988).
- <sup>38</sup> B. J. van Wees, H. van Houten, C. W. J. Beenakker, J. G. Williamson, L. P. Kouwenhoven, D. van der Marel and C. T. Foxon, *Phys. Rev. Lett.* **60**, 848 (1988).
- <sup>39</sup> B. J. van Wees, L. P. Kouwenhoven, E. M. M. Willems, C. J. P. M. Harmans, J. E. Mooij, H. van Houten, C. W. J. Beenakker, J. G. Williamson and C. T. Foxon, *Phys. Rev. B* **43**, 12431 (1991).
- <sup>40</sup> D.C. Glattli, *Eur. Phys. J. Special Topics* **172**, p. 163 (2009).
- <sup>41</sup> F.D. Parmentier, A. Mahé, A. Denis, J.-M. Berroir, D.C. Glattli, B. Plaças and G. Fève, *Rev. Sci. Instrum.* **82**, p. 013904 (2011).
- <sup>42</sup> S. Cova, M. Ghioni, A. Lacaita, C. Samori and F. Zappa, *Applied Optics* **35**, p. 1956 (1996).
- <sup>43</sup> D. Golubev and A. Zaikin, *Phys. Rev. B* **59**, 9195 (1999).
- <sup>44</sup> J. Von Delft, *Int. J. Mod. Phys. B* **22**, 727 (2008).
- <sup>45</sup> C. Altimiras, H. le Sueur, U. Gennser, A. Cavanna, D. Mailly and F. Pierre, *Nature Physics* **6**, p. 34 (2010).
- <sup>46</sup> S. Deléglise, I. Dotsenko, C. Sayrin, J. Bernu, M. Brune, J.-M. Raimond and S. Haroche, *Nature* **455**, p. 510 (2008).
- <sup>47</sup> D. T. Smithey, M. Beck, M. G. Raymer and A. Faridani, *Phys. Rev. Lett.* **70**, p. 1244 (1993).
- <sup>48</sup> A. I. Lvovsky and M. G. Raymer, *Rev. Mod. Phys.* **81**, 299 (2009).
- <sup>49</sup> R. Twiss, A. Little and R. Hanbury Brown, *Nature* **180**, 324 (1957).
- <sup>50</sup> U. Fano, *Am. J. Phys.* **29**, p. 539 (1961).
- <sup>51</sup> M. Henny, S. Oberholzer, C. Strunk, T. Heinzel, K. Ensslin, M. Holland and C. Schönenberger, *Science* **284**, p. 296 (1999).
- <sup>52</sup> W. Oliver, J. Kim, R. Liu and Y. Yamamoto, *Science* **284**, p. 299 (1999).
- <sup>53</sup> R. Liu, B. Odom, Y. Yamamoto and S. Tarucha, *Nature* **391**, p. 263 (1998).
- <sup>54</sup> G. Baym, *Acta Physical Polonica B* **29**, p. 1839 (1998).

- <sup>55</sup> T. Jeltès, J. McNamara, W. Hogervorst, W. Vassen, V. Krachmalnicoff, M. Schellekens, A. Perrin, C. Hong, D. Boiron, A. Aspect and C. Westbrook, *Nature* **445**, p. 402 (2007).
- <sup>56</sup> G. Fève, P. Degiovanni and T. Jolicoeur, *Phys. Rev. B* **77**, p. 035308 (2008).
- <sup>57</sup> C. Hong, Z. Ou and L. Mandel, *Phys. Rev. Lett.* **59**, p. 2044 (1987).
- <sup>58</sup> J. Beugnon, M. Jones, J. Dingjan, B. Darquié, G. Messin, A. Browaeys and P. Grangier, *Nature* **440**, p. 779 (2006).
- <sup>59</sup> C. Grenier, R. Hervé, E. Bocquillon, F.D. Parmentier, B. Plaçais, J.-M. Berroir, G. Fève and P. Degiovanni, Single electron quantum tomography in quantum hall edge channels, arXiv:1010.2166.
- <sup>60</sup> S. Ol'khovskaya, J. Splettstoesser, M. Moskalets and M. Büttiker, *Phys. Rev. Lett.* **101**, p. 166802 (2008).
- <sup>61</sup> M. Moskalets and M. Büttiker, *Phys. Rev. B* **83**, p. 035316 (2011).
- <sup>62</sup> J. Splettstoesser, M. Moskalets and M. Büttiker, *Phys. Rev. Lett.* **103**, p. 076804 (2009).
- <sup>63</sup> P. Roulleau, F. Portier, D.C. Glattli, P. Roche, A. Cavanna, G. Faini, U. Gennser and D. Mailly, *Phys. Rev. B* **76**, p. 161309 (2007).
- <sup>64</sup> P. Roulleau, F. Portier, P. Roche, A. Cavanna, G. Faini, U. Gennser and D. Mailly, *Phys. Rev. Lett.* **101**, p. 186803 (2008).
- <sup>65</sup> I. Neder, F. Marquardt, M. Heiblum, D. Mahalu and V. Umansky, *Nature Physics* **3**, p. 534 (2007).
- <sup>66</sup> H. Le Sueur, C. Altimiras, U. Gennser, A. Cavanna, D. Mailly and F. Pierre, *Phys. Rev. Lett.* **105**, p. 056803 (2010).
- <sup>67</sup> C. Altimiras, H. Le Sueur, U. Gennser, A. Cavanna, D. Mailly and F. Pierre, *Phys. Rev. Lett.* **105**, p. 226804 (2010).
- <sup>68</sup> D. Pines and P. Nozières, *The theory of quantum liquids* (Perseus Book, 1966).
- <sup>69</sup> P. Degiovanni, C. Grenier and G. Fève, *Phys. Rev. B* **80**, p. 241307(R) (2009).
- <sup>70</sup> P. Degiovanni, C. Grenier, G. Fève, C. Altimiras, H. le Sueur and F. Pierre, *Phys. Rev. B* **81**, p. 121302(R) (2010).
- <sup>71</sup> I. Safi and H. Schulz, *Phys. Rev. B* **52**, p. R1740 (1995).
- <sup>72</sup> I. Safi and H. Schulz, Transport through a single band wire connected to measuring leads, in *Quantum Transport in Semiconductor Submicron Structures*, ed. B. Kramer (Kluwer Academic Press, Dordrecht, 1995).
- <sup>73</sup> M. Büttiker, A. Prêtre and H. Thomas, *Phys. Rev. Lett.* **70**, p. 4114 (1993).
- <sup>74</sup> A. Prêtre, H. Thomas and M. Büttiker, *Phys. Rev. B* **54**, p. 8130 (1996).
- <sup>75</sup> S. Nigg, R. López and M. Büttiker, *Phys. Rev. Lett.* **97**, p. 206804 (2006).
- <sup>76</sup> C. Mora and K. Le Hur, *Nature Physics* **6**, p. 697 (2010).
- <sup>77</sup> Y. Hamamoto, T. Jonckheere, T. Kato and T. Martin, *Phys. Rev. B* **81**, p. 153305 (2010).
- <sup>78</sup> S. Nigg and M. Büttiker, *Phys. Rev. B* **77**, p. 085312 (2008).
- <sup>79</sup> Z. Ringel, Y. Imry and O. Entin-Wohlman, *Phys. Rev. B* **78**, p. 165304 (2008).
- <sup>80</sup> J. Gabelli, G. Fève, J.-M. Berroir, B. Plaçais, A. Cavanna, B. Etienne, Y. Jin and D.C. Glattli, *Science* **313**, p. 499 (2006).
- <sup>81</sup> J. Gabelli, G. Fève, T. Kontos, J.-M. Berroir, B. Plaçais, D.C. Glattli, B. Etienne, Y. Jin and M. Büttiker, *Phys. Rev. Lett.* **98**, p. 166806 (2007).
- <sup>82</sup> R. Ionicioiu, G. Amaratunga and F. Udrea, *Int. J. Mod. Phys. B* **15**, p. 125 (2001).
- <sup>83</sup> I. Levkivskiy and E. Sukhorukov, *Phys. Rev. B* **78**, p. 045322 (2008).
- <sup>84</sup> A. M. Lunde, S. E. Nigg and M. Büttiker, *Phys. Rev. B* **81**, p. 041311(R) (2010).
- <sup>85</sup> D. Kovrizhin and J. Chalker, Equilibration of integer quantum hall edge states, arXiv:1009.4555.
- <sup>86</sup> G. Seelig and M. Büttiker, *Phys. Rev. B* **64**, p. 245313 (2001).
- <sup>87</sup> H. Forster, S. Pilgram and M. Büttiker, *Phys. Rev. B* **72**, p. 075301 (2005).
- <sup>88</sup> V.-W. Chung, P. Samuelsson and M. Büttiker, *Phys. Rev. B* **72**, p. 125320 (2005).
- <sup>89</sup> J. Chalker, Y. Gefen and M. Veillette, *Phys. Rev. B* **76**, p. 085320 (2007).
- <sup>90</sup> C. Neuenhahn and F. Marquardt, *Phys. Rev. Lett.* **102**, p. 046806 (2009).
- <sup>91</sup> C. Neuenhahn and F. Marquardt, *New Journal of Physics* **10**, p. 115018 (2008).
- <sup>92</sup> I. Neder and F. Marquardt, *New Journal of Physics* **9**, p. 112 (2007).
- <sup>93</sup> D. L. Kovrizhin and J. T. Chalker, *Phys. Rev. B* **80**, p. 161306 (2009).
- <sup>94</sup> D. L. Kovrizhin and J. T. Chalker, *Phys. Rev. B* **81**, p. 155318 (2010).
- <sup>95</sup> I. P. Levkivskiy and E. V. Sukhorukov, *Phys. Rev. Lett.* **103**, p. 036801 (2009).
- <sup>96</sup> D. B. Gutman, Y. Gefen and A. D. Mirlin, *Phys. Rev. B* **81**, p. 085436 (2010).
- <sup>97</sup> D. Gutman, Y. Gefen and A. Mirlin, *Europhys. Lett.* **90**, p. 37003 (2010).
- <sup>98</sup> I. Snyman and Y. Nazarov, *Phys. Rev. B* **77**, p. 165118 (2008).
- <sup>99</sup> C. Bauerle, P. Degiovanni and L. Saminadayar, *Int. J. Nanotechnol* **7**, p. 403 (2010).